X-ray spectroscopy and quantification of an AlCuLi quasi-crystal: A step forward for combination of reflection zone plate and crystal spectrometers

Khalil Hassebi, Nicolas Rividi, Omar Boudouma, Michel Fialin, Karine Le Guen, Philippe Jonnard

X-ray spectroscopy and quantification of an AlCuLi quasi-crystal: a step forward for combination of reflection zone plate and crystal spectrometers

Khalil Hassebi[1], Nicolas Rividi[2], Omar Boudouma[3], Michel Fialin[2], Karine Le Guen[1], Philippe Jonnard[1]

(1) Laboratoire de Chimie Physique—Matière et Rayonnement, Faculté des Sciences et Ingénierie, Sorbonne Université, UMR CNRS, 4 place Jussieu, 75252 Paris Cedex 05, France

(2) Service Camparis, UAR 3455 —CNRS, OSU Ecce Terra, Sorbonne Université, 4 place Jussieu, 75005 Paris, France

(3) CNRS-INSU, Institut des Sciences de la Terre de Paris, ISTeP, 75005 Paris, France

Abstract

We present the analysis of an AlCuLi quasi-crystal on through electron probe microanalyzer equipped with spectrometers working both in the soft and ultra-soft x-ray ranges. This original combination enables obtaining the Li Kα and Al $L_{2,3}$ emissions with a reflection plate spectrometer and the Al Kβ and Cu Lα emissions with a curved-crystal spectrometer. All these emissions are emission bands, sensitive to the chemical state of the emitting element. From the observation of the valence band shapes, it is confirmed that the electronic structure of the quasi-crystal is quite different from that of the corresponding pure metals. From the measured intensities, quantification is performed using the PAP model. The weight fractions calculated from the ultra-soft x-ray emission intensities are very dependent on the chosen database of mass attenuation coefficients. Comparison with fractions calculated with small uncertainty in the soft x-ray range enables choosing which databases are the most relevant for the ultra-soft x-ray range. Both quantifications performed from ultra-soft and soft x-ray emissions are compatible, leading to the $Al_{60}Cu_{24}Li_{16}$ weight concentration of the quasi-crystal.

Keywords

x-ray emission spectroscopy ; elemental quantification ; quasi-crystal ; Li K emission ; electron probe microanalysis ; reflection zone plate ; mass attenuation coefficient ; ultra-soft x-rays ; x-ray emission band

Corresponding author

Dr. Philippe Jonnard, philippe.jonnard@sorbonne-universite.fr

Introduction

Direct characterization of light elements emitting within the ultra-soft x-ray range (30 – 150 eV) by x-ray emission spectroscopy (XES) remains challenging and crucial in various fields of science or industry. In this context, lithium is one of the most interesting elements as it stays outside the field of the common XES devices like electron microscopes or probes. Development of dedicated spectrometers for the ultra-soft x-ray range [1,2] and designed to work with electron beam apparatus, electron microscopes and electron microprobes, gives the opportunity to extend analytical capabilities from ultra-soft to soft x-rays with the same technics. Thus it is now possible to track the Li Kα ($2p$ – $1s$ transition) [3–5] together with elements in which x-rays arise at higher energy and to analyse many elements in different x-ray spectral domains. Moreover, these spectrometers offer a relatively high resolving power, E/ΔE about equal to 100 or larger. Thus, they enable to improve the analysis of emissions falling in the soft x-ray domain (150 – 5000 eV) and particularly in the 150 – 750 eV energy range generally measured with crystal spectrometers equipped with periodic multilayers giving a poor resolving power, E/ΔE about equal to 15 or larger. The high spectral resolution is strongly required for the study of emission bands (transitions between the occupied valence states towards a core level) since their shape and precise energy position are highly dependent on the chemical state of the emitting element. For example, the combination of observations obtained by XES and electron energy loss spectroscopy [1], made it possible to give evidence of the pseudo-gap present between the occupied and unoccupied valence states in quasi-crystals.

The ultra-soft x-ray spectrometers also enable making intensity measurements and thus open the possibility to perform elemental quantification [6], *i.e.* to determine the weight fraction of an element within a solid material from the intensity of its characteristic emission. The combination of this quantification with the one performed in a standard way with the crystal spectrometers of the electron microprobe is beneficial because:

- coherent determinations obtained in two independent spectral ranges validate the quantification;
- discrepancies between the two determinations point to discrepancies in fundamental parameters used in the quantification model; particularly the tabulated values of the attenuation coefficients in the ultra-soft x-ray range are not known with accuracy [7,8].

In this work, we explore in an original way an AlCuLi quasi-crystal, by combining spectra obtained in the ultra-soft x-ray range with a reflection zone plate (RZP) spectrometer [2,5] and those obtained in the soft x-ray range with a standard Johann-type curved crystal spectrometer [9,10]. RZP are diffractive and focusing optics working as two-dimensional variable line spacing gratings [11] to disperse x-rays. The Li Kα and Al $L_{2,3}$ ($3sd$ – $2p_{1/2,3/2}$ transition) spectra are obtained with the RZP spectrometer; the Al Kα ($2p$ – $1s$ transition), Al Kβ ($3p$ – $1s$ transition) and Cu Lα ($3d$ – $2p_{3/2}$ transition) spectra are obtained with a crystal spectrometer. Together, they give an insight on the electronic structure of this quasi-crystal, confirmed by the comparison with previously obtained emissions bands. Indeed, quasi-crystals present unexpected translation symmetries [12] which lead to electronic properties different to the ones of mere metallic alloys [13,14].

Moreover, quantification is performed in both ultra-soft and soft x-ray ranges. However, with our current setup, it is not possible to run at the same time the crystal and RZP spectrometers to combined intensity measurements obtained in both spectral ranges. Then, in the ultra-soft x-ray range, the determination of the Li Kα and Al $L_{2,3}$ intensities enables calculating the lithium and aluminium weight fractions and deducing the one of copper by difference. In the soft x-ray range, where lithium does not

emit, the determination of the Al (from the Al Kα emission) and copper weight fractions enables calculating the lithium weight fraction.

Experimental details and preliminary chemical characterizations

The AlCuLi studied quasi-crystalline sample was fabricated in the 1990s, a few years after the surprising discovery of quasi-crystals presenting unexpected diffractive properties [12,15]. The sample consists of quasi-crystalline phases pressed in a lead matrix. Prior to the introduction of the sample in the analysis chamber, a cleaning of its surface was performed using an argon ion beam under a glancing angle of 20°. The ion bombardment duration was 30 minutes at 3 kV followed by 30 minutes at 2.5 kV. After cleaning, the sample was stored in nitrogen atmosphere and spent a few minutes in air during its transfer inside the electron microprobe. As the sample is not an insulator, no conductive carbon coating of its surface was necessary avoiding further on the final spectrum.

A first characterization was performed on a scanning electron microscope (Zeiss Supra) using 15 keV incident electron beam to determine the precise location of quasi-crystal fragments suitable for x-ray analysis as seen on the backscattering electron image of Figure 1. Consequently, the quasi-crystal low-density phases appear as dark zones, 10 µm to some 100 µm long, surrounded by the large and light grey leaded matrix.

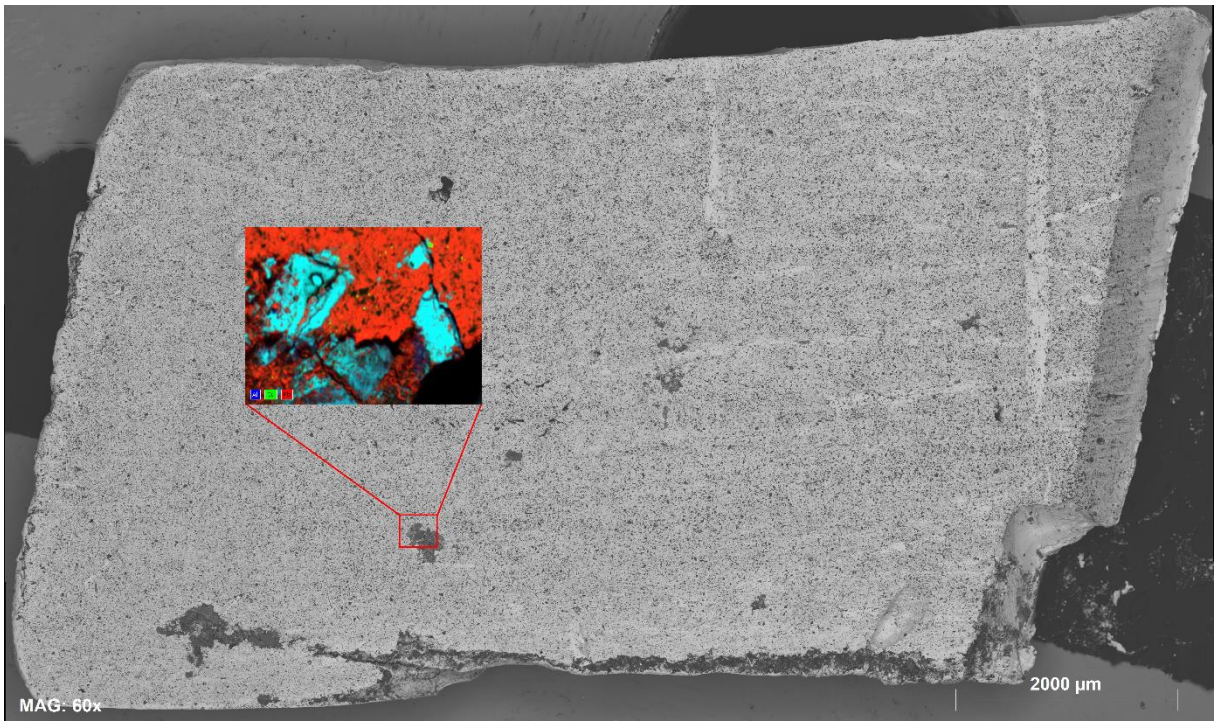

Figure 1: Backscattered electron mosaic-type image of the AlCuLi quasi-crystal sample obtaine at high magnification. The red square is indicating zone analysed in the following. The colour inset is the x-ray image of the analysed zone showing the AlCuLi quasi-crystal (light blue region, Al K emission and Cu L emissions) and the Pb matrix (red, Pb Mα emission).

Figure 2(a) presents the BSE image of the analysed zone, obtained with 5 keV electrons. It is more or less rectangular and has a size of about 55 µm and was selected because of its flat and smooth surface, required to perform analysis by electron probe micro analyser (EPMA). Chemical maps extracted from a unique hyperspectral image obtained by energy dispersive spectrometry with a silicon drift detector (SDD, Bruker) in the ranges of the Al Kα, Cu Lα , and O Kα x-ray emissions are shown in Figures 2(b), (c) and (d) respectively. The SDD used in this study cannot reach lithium spectral range. A colour

composite image was obtained by the combination of the three spectral images and is shown as the colour inset of Figure 1.

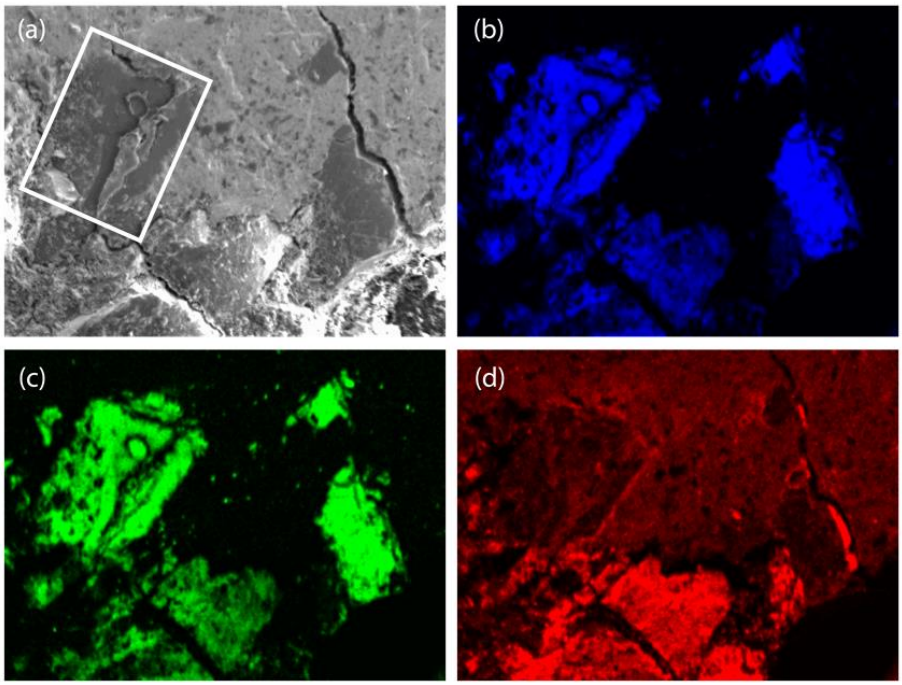

Figure 2: (a) BSE image and (b) Al Kα, (c) Cu Lα and (d) O Kα spectral images of the analysed zone. The analysed zone is inside the white rectangle. The size of the images is 120 µm x 190 µm.

The wavelength dispersive spectra of the different elements present in the sample were obtained with a CAMECA SX100 EPMA, operating at 5 kV and 40 nA. This acceleration voltage was chosen as a compromise to obtain a well-defined and well-controlled electron beam having a diameter below 1 µm and to optimize the analysed thickness with the Li Kα emission band. The electron current was defined as a compromise between possible beam damage and acquisition time. During analysis, the experimental chamber is at a pressure of a few 4 x 10^{-6} mbar.

The RZP spectrometer (WDSX from NOB, Nano Optics Berlin) implemented on the CAMECA microprobe [5], enabled to scan the emitted photon energies between 40 and 120 eV. This spectrometer works as a variable line spacing grating spectrometer, focusing the x-rays on a line to obtain the spectra with a CCD camera, that is to say working as a flat-field spectrometer. The spectrum of the quasi-crystal in the full range of the spectrometer presented in Figure 3(a)results of the sum of 17 acquisitions (18 were performed, the 12th is lost) of 100 s performed at the same location. Various features are observed and labelled from #1 to #11, the more interesting ones being the Li Kα (#3) and Al $L_{2,3}$ (#5, 6) emissions. The other features are related to the C Kα (#2, 9) and O Kα (#8, 10) emissions diffracted at the high orders of the RZP. Carbon and oxygen are originating from the thin contamination layer at the surface of the sample following its transfer in air. Some background locations are also numbered (#1, 4, 7, 11). We have checked the stability of the analysed zone under the electron beam by plotting in Figures 3(b) and (c) the number of counts measured at some of the various labelled positions as a function of the 17 acquisitions. Both peaks and backgrounds are stable; only a 10% decrease in the number of counts occurs after the first 100-200 s. Other quasi-crystalline zones of the sample were also analysed and revealed being unstable under the electron bombardment: after a few hundred seconds, the intensity of the lithium and aluminium emissions decreases while the one of carbon increases.

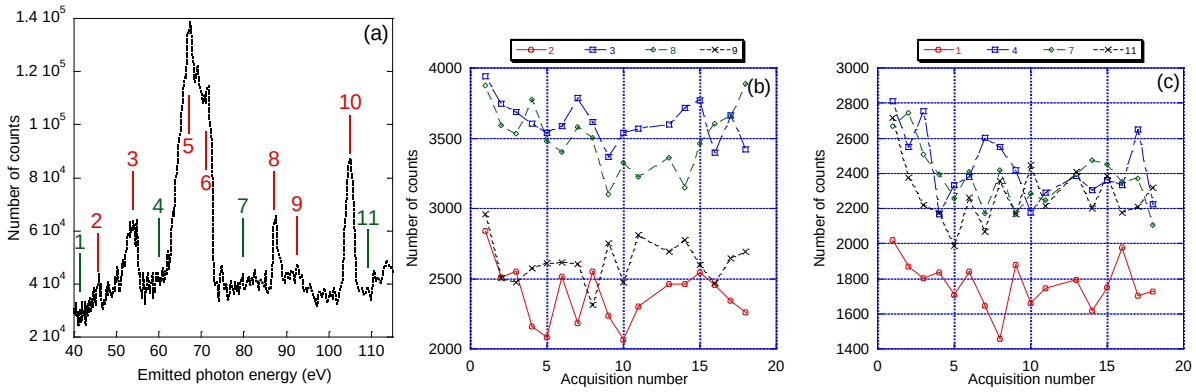

Figure 3: (a) Spectrum of the quasi-crystal obtained in the full range of the RZP spectrometer where different peak (in red) and background (in green) locations are labelled; (b) follow up of the number of counts measured at the peak locations labelled in (a) as a function of the acquisition number; (c) follow up of the number of counts measured at the background locations labelled in (a).

A Johann-type curved-crystal x-ray spectrometer equipped with a TlAP (001) crystal (2d = 2.5745 nm) was used to disperse soft x-rays and acquire the Al Kα, Al Kβ, and Cu Lα emissions. The incident electron beam was set to 5 kV and 40 nA. Spectra were obtained at the first diffraction order except for Al Kβ at the second order to improve the spectral resolution. In this last case, five spectra, resulting from 30 accumulations of the Al Kβ emission band, for a total time of 5 hours, were acquired at the same location and summed as only a small decrease (less than 10%) of the intensity was observed as a function of the electron irradiation time.

The Monte Carlo program McXray [16] was used to calculate the depth distribution of the ionizations inside a AlCuLi material having a density of 2.2 g.cm^{-3}. It is found that the maximum depth of the ionization is 400 nm for the Li K (1*s*) core level having the lowest binding energy and 350 nm for the Al K core level having the highest binding energy. Then using the attenuation coefficients taken from CXRO [17] and the take-off angle (40°) of the emitted radiation in the EPMA, the maximum thickness from where the characteristic x-rays can come from is estimated to 350 nm. Increasing the density to 4 g.cm^{-3} decreases the thicknesses given above by a factor of 2. Thus, under the 5 keV electron irradiation, a few hundreds of nanometers are probed, *i.e.* the bulk of the quasi-crystal is analysed.

Quantification was performed both in the ultra-soft x-ray range with the RZP spectrometer using the Li Kα and Al $L_{2,3}$ emissions and in the soft x-ray range with the crystal spectrometer using the Al Kα and Cu Lα emissions. As it is not possible to detect the Cu $M_{2,3}$ emission or to observe the Cu Lα emission with the RZP spectrometer, the copper mass fraction was determined by difference. That is to say, the Cu weight fraction is calculated as the difference between 1 (100%) and the sum of the Li and Al fractions. As it is not possible to observe the Li Kα emission with a crystal spectrometer, in this case the lithium mass fraction was obtained by difference. Pouchou and Pichoir (PAP) model [18,19], which corrects various matrix effect like absorption or fluorescence, was used to perform quantification. The values of mass absorption coefficients (MAC) are taken from the databases MAC30 [20], Chantler [21], EPDL97 [22], PENELOPE 2018 [23] or EPDL 2023 [24]. Because the absorption is large in the ultra-soft x-ray range, it is necessary that the sample be polished so that a plane and smooth surface of the sample is obtained.

Results and discussion

Spectrum treatment

The spectrum of the AlCuLi quasi-crystal is presented in Figures 3(a) and 4. The Li Kα and Al $L_{2,3}$ emissions are partly interfering with the C Kα and O Kα emissions diffracted at high orders. These carbon and oxygen contributions, coming from surface contamination, need to be removed in order to get spectra comparable to those found in the literature and to determine the integrated intensities that will be used in the quantification process.

Energies and relative intensities of the various diffraction orders of the C Kα and O Kα emissions have been determined from reference spectra obtained with graphite and magnesium oxide under the same analytical conditions. On the quasi-crystal spectrum, we note that the C Kα emission at 47.5 eV (6^{th} diffraction order, see Figure 4) and O Kα emission at 105 eV (5^{th} diffraction order, see Figure 3) are free of spectral interference. These characteristic emissions were extracted and reproduced at the various orders occurring in the spectral range of the Li Kα and Al $L_{2,3}$ emissions (4^{th} and 5^{th} for carbon; 7^{th}, 8^{th}, 9^{th} and 10^{th} for oxygen) by applying the relative intensities between the various orders and calculating their new energy by multiplying the initial photon energies by the ratio of the diffraction orders. The result is shown in Figure 4 in the spectral range of interest, 40 – 80 eV, where a linear background is subtracted and where the number of counts is normalized to 1 s and 1 nA. Oxygen does not contribute significantly whereas the carbon contribution is not negligible, particularly in the Li Kα range where it is a little less than 20%.

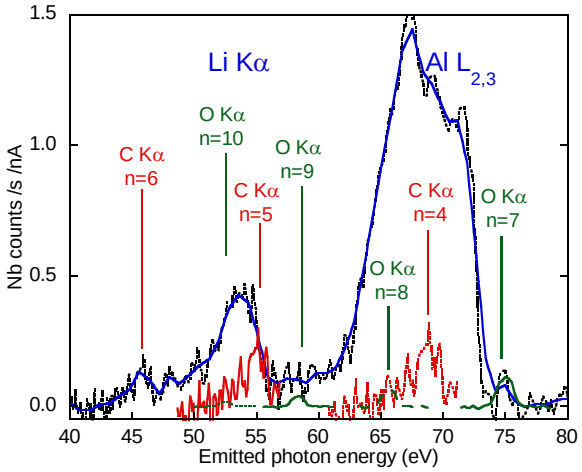

Figure 4: Li Kα and Al $L_{2,3}$ range of the quasi-crystal (black line and blue line for the smoothed spectrum) on which are superimposed the C Kα (red lines) and O Kα (green lines) emissions diffracted at various higher orders noted as *n*. The number of counts is normalized for 1 s and 1 nA.

Comparison of the emission bands with previous studies

The AlCuLi phase was not the most studied quasi-crystal; however it is possible to retrieve in the literature its Li Kα and Al $L_{2,3}$ emission bands [25] as well as its Al Kβ and Cu Lα emission bands [26]. In both studies, the characteristic emissions were generated under electron irradiation, at 3 keV in Ref. [25] and 2.5 or 3 keV in Ref. [26].

The high order contributions of the C Kα and O Kα emissions shown in Figure 4 are subtracted from the Li Kα and Al $L_{2,3}$ emission bands obtained with the RZP spectrometer. Corrected emissions are plotted in Figure 5 in comparison to the emissions obtained with a grating spectrometer [25]. Spectra obtained in the framework of this study and published spectra are in good agreement regarding

photon energy, bandwidth and band shape. Thus, we confirm that we observe the Li *p* and Al *sd* local and partial valence density of states in the AlCuLi quasi-crystal.

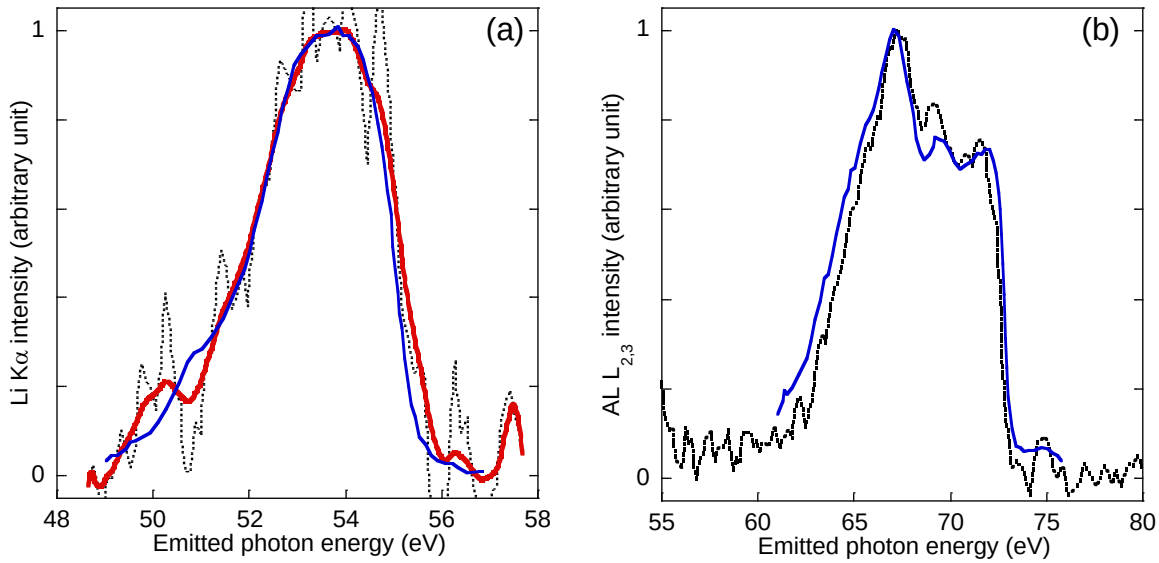

Figure 5: Li Kα (a) and Al $L_{2,3}$ (b) emission bands of the AlCuLi quasi-crystal obtained with the RZP spectrometer (red line) and compared to spectra given in the literature [25] (blue line). In (a) the black line is the spectrum obtained from the data treatment to remove high orders peaks and the red line is the corresponding smoothed spectrum. Spectra are normalised to their maximum.

The Li Kα and Al $L_{2,3}$ emission bands of the quasi-crystal and of pure Li and Al metals are compared in Figure 6. They were treated in the same way as the quasi-crystal spectrum to remove the high-diffracted orders of the carbon and oxygen emissions. Details of the preparation of the lithium sample are given in Ref. [5]. As expected, the metal spectra are characterised by a marked drop in intensity at the Fermi level occurring at the top of valence band. It can be noted that the shapes of the spectra of pure metals are similar as those of an AlCuLi metal alloy [4]. The shapes of the emission bands of the quasi-crystal are well different from the ones of the pure metals as they present different energies of their maximum and quite different bandwidths. These differences are related to the different energy distributions of occupied states in the valence bands of these two kinds of materials [27,28].

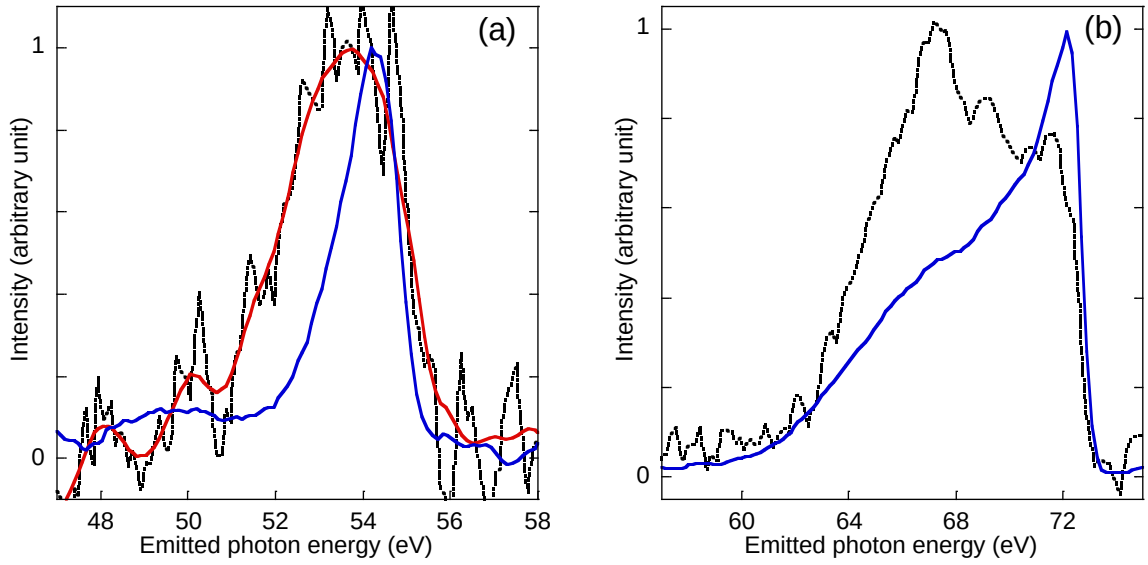

Figure 6. Li Kα (a) and Al $L_{2,3}$ (b) emission bands of the AlCuLi quasi-crystal (black dashed lines and red line for the smooth lithium spectrum) and of pure Li and Al metals (blue solid lines). Spectra are normalized to their maximum.

Spectra measured in the soft x-ray range with the TlAP crystal are compared to the Al Kβ and Cu Lα spectra measured with a Johann-type x-ray spectrometer [26] in Figure 7. Both the present and the published spectra are in good agreement regarding position, bandwidth and band shape. However, the Cu Lα emission band obtained in this work presents some extra intensity above the Fermi level, *i.e.* at photon energies above 932 eV. We assume that this is due to more intense Coster-Kronig satellites (satellites coming from multiple ionization of the Cu atoms) [10] because in our work we probably used a higher energy of incident electrons. The good agreement between our work and the published spectra confirms that we observe the Al *p* and Cu *d* local and partial density of states in the AlCuLi quasi-crystal.

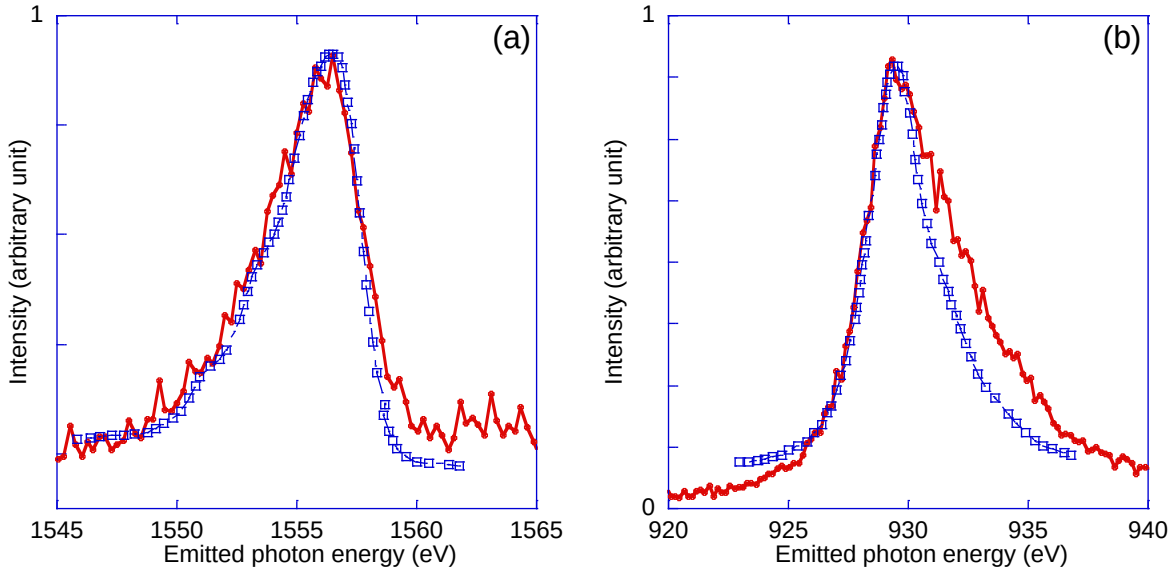

Figure 7: Al Kβ (a) and Cu Lα (b) of the AlCuLi quasi-crystal measured with a TlAP crystal (red line) and compared to spectra given in the literature [26] (blue line). Spectra are normalised to their maximum.

Quantification

The reference materials to perform quantification were pure Al and Li metals for the ultra-soft x-ray range (Figure 6) and Al and Cu metals for the soft-x-ray range. In the ultra-soft x-ray range, the integrated intensities, *i.e.* the area under the Li Kα and Al $L_{2,3}$ emissions were taken into account. The emissions of Al and Li metals have been treated in the same way as the quasi-crystal spectrum to remove the high order diffracted emissions. Conversely in the soft x-ray range, the number of counts at the peak maximum of both the Al Kα and the Cu Lα emissions were measured as a common usage for EPMA.

From the integrated intensities of the Li Kα and Al $L_{2,3}$ emissions measured for the references and the quasi-crystal, the weight fractions are determined using the PAP model [18]. Table 1 collects the weight fractions calculated with mass attenuation coefficients extracted from the five databases. The results vary strongly with the chosen database, by a factor 2 for both the Li and Cu fractions and by 50% for the Al fraction.

MAC database	*Ultra-soft x-ray range*

	Al (wt%) / (at%)	*Li (wt%)/ (at%)*	*Cu (wt%)/ (at%)*
MAC30	74.2 / 52.7	16.2 / 44.5	9.4 / 2.8
Chantler	49.6 / 35.6	19.8 / 55.1	30.5 / 9.3
EPDL97	51.2 / 37.2	19.1 / 53.7	29.6 / 9.1
PENELOPE 2018	57.3 / 39.1	20.7 / 54.6	21.9 / 6.3
EPDL 2023	63.8 / 51.6	12.9 / 40.4	23.2 / 8.0
	Soft x-ray range		
MAC30	59.6 / 44.1	16.9 / 48.3	23.5 / 7.5

Table 1: Weight fractions and atomic concentrations for the AlCuLi quasi-crystal calculated from the Li Kα and Al $L_{2,3}$ intensities and with MAC from different databases. The Cu weight fraction is determined by difference. The last line gives the weight fractions determined from the Al Kα and Cu Lα intensities in the soft x-ray range. In this case, the Li weight fraction is calculated by difference.

Quantification for the emissions in the soft x-ray range was performed on 20 points along a 30 µm-long line located on a fresh part of the analysed zone, Figure 2(a). Figure 8 shows the Al, Cu, and Li weight fractions determined at the 20 measured spots. In this quantification, the MAC30 database is used. The four databases indicated in Table 1 have quite similar MAC with a relative difference between them of less or equal to 1% in the Al Kα and Cu Lα ranges There is a large variation of the fractions according to the position of the electron beam. We assume that this is due to a variation in the incidence of the electron beam on the quasi-crystal surface, following the difficult polishing of the surface where are present two materials (Pb matrix and quasi-crystals). For the subsequent analysis, we remove the first and last points of the line as well as the points #8 and #9, presenting quite low Al fractions. The calculated weight fractions in the AlCuLi quasi-crystal are the following: Al 59.6 ± 2.0 wt.%, Cu 23.5 ± 0.9 wt.%, and Li 16.4 ± 2.9 wt.% (Table 1), where the indicated uncertainty represents the standard deviation for the 16 considered measurements. Note that this uncertainty of about 3% for Al is larger than the commonly accepted uncertainty, *i.e.* 1%, for EPMA measurements.

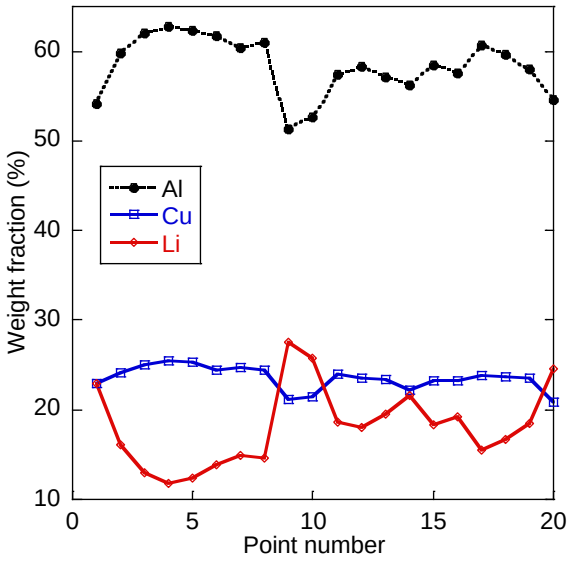

Figure 8: Weight fractions for the AlCuLi quasi-crystal calculated from the Al Kα and Cu Lα intensities on 20 different points of the analysed zone. The Li weight fraction is determined by difference.

The main information that we can extract from the results in Table 1 is that the Li fraction, either effectively obtained from the Li Kα and the Al $L_{2,3}$ emissions, except those based on the MAC30 database, or deduced from the difference to 100% from the Al Kα and Cu Lα emissions in the soft x-ray range, are broadly consistent from each other. Indeed, between the results obtained from either

procedure we note a difference of ± 10 wt.% for Al, ± 6 wt.% for Cu and ± 4 wt.% for Li, since parameters in the PAP model for Li Kα data reduction are certainly not still fully constrained. Moreover, if we consider the mean weight fractions calculated without the MAC30 database in the ultra-soft x-ray range, the differences with the fractions calculated in the soft x-ray range are limited to ± 4 wt.% for Al, ± 1 wt.% for Cu and ± 2 wt.% for Li

The uncertainty related to quantification in the ultra-soft x-ray range comes in part from the uncertainties on the measured intensities of both Li Kα and Cu Lα emissions in the quasi-crystal and the reference materials. The different factors that can have an impact on the determination of the collected intensities in the ultra-soft x-ray range are:

- the difficult polishing of the sample making the electron beam not perfectly perpendicular to the sample surface;
- the background subtraction;
- the subtraction of the C Kα and O Kα high-order emissions;
- the contribution of peak overlapping; both Cu $M_{2,3}$ and Al $L_{2,3}$ emissions are located in the same photon energy range [29]; however the Cu $M_{2,3}$ emission is very weak and in our experimental conditions its integrated intensity is estimated to be less than 1% of the Al $L_{2,3}$ intensity of the quasi-crystal;
- the attenuation of the radiation emitted inside the quasi-crystal by the surface contamination ; if we consider a carbon oxide being 1 nm thick and 2 g/cm^3 dense, 2% of the Li Kα outgoing intensity and 3% of the Al $L_{2,3}$ intensity are absorbed;
- the plasmon satellite of the Al $L_{2,3}$ emission; this satellite which represents 3% of the intensity of the main band, is shifted by 17 eV [30] toward lower photon energies and thus is located in the range of the Li Kα emission band.

Thus, we estimate the uncertainty on the intensities to ±10% which propagates to 14% on the k-ratios, the ratios of the intensities measured on the sample to the one measured on the reference materials. This translates to an uncertainty on the Li and Al fractions of ± 2 wt.% and ± 5 wt.% respectively. Thus, the weight fractions determined in both spectral ranges are compatible, see Table 1. These uncertainties do not account for the uncertainties associated with the atomic parameters used in the PAP model.

Conclusion and perspectives

The original setup combining a commercial EPMA and RZP spectrometer allowed obtaining the Li Kα emission band from an AlCuLi quasi-crystal, despite some interferences coming from the C Kα and O Kα emissions diffracted at high orders of the RZP. From the collected intensity, about one count /s /nA, we expect to detect Li with mass concentration as low as 1% in our experimental conditions, 5 kV and 40 nA. In the future, it will be possible to improve the present performances of the spectrometer by scanning the electron beam on the sample surface while acquiring ultra-soft x-ray spectra and by changing the RZP to another one working in a geometry attenuating strongly the high-order diffracted emissions.

Reflection zone plate and crystal spectrometers implemented in electron microprobes are complementary tools to characterize solid materials. Their combination enables obtaining a quite complete view of the electronic structure, *i.e.* the local (element dependent) and partial (symmetry dependent) density of states, of the AlCuLi quasi-crystal. Thus, the Al and Li spectra are far from those of the pure metals or an AlCuLi alloy, but in agreement with those of previously studied quasi-crystals.

The good spectral resolution of the RZP opens the possibility to identify the chemical state of lithium atoms directly from the observation of the Li Kα emission band [31,32].

Elemental quantification was performed in both ultra-soft and soft x-ray ranges. Using both kinds of spectrometers makes possible to determine the intensities emitted by only two of the three elements and by combination enables the weight fraction calculation of the three elements occurring in the quasi-crystal. The weight fractions obtained from the soft-x-ray range intensities are calculated with a 3% uncertainty. This uncertainty would have decreased if the analysis would have been performed on a sample of certified composition. The soft x-ray determination helps to decide among the available mass absorption databases which one is relevant to use in the ultra-soft x-ray range. The uncertainty on the weight fractions obtained in the ultra-soft x-ray range are still too large, owing to large uncertainties on the collected intensities. However, the mass composition of the quasi-crystal is close to $Al_{60}Cu_{24}Li_{16}$, corresponding to an $Al_{44}Cu_8Li_{48}$ atomic composition. The AlCuLi quasi-crystalline phase exists in a limited range of concentration of its elements. Our determined value is a bit far from the concentration of the phase $Al_{56}Cu_{10}Li_{34}$indicated by Bruhwiler *et al.* [25], but rather close to the weight fractions of some phases indicated in the literature, $Al_{60}Cu_{30}Li_{10}$ [26], $Al_{64.4}$ $Cu_{27.0}Li_{8.6}$ [33], $Al_{62.8}Cu_{28.0}Li_{9.1}$ [34] and $Al_{65.7}Cu_{25.8}Li_{8.5}$ [35]. This comparison makes us confident that we really observe and quantify an AlCuLi quasi-crystal. The observed deviation of the composition could arise because the tiny, non-equilibrium crystal in the present study may not have the ideal bulk composition.

Despite promising results, our current setup is not yet optimized for the accurate quantification of lithium, as several critical factors limit the precision of our measurements, the present detection limit of lithium being a few weight percent if shorter acquisition times or electron currents would be used. Several aspects can be improved to design a complete and routine-like ultra-soft x-ray quantification setting. Beam scanning together with interference removal (high order and first order interferences) and cryogenic sample holder are thought to be the most promising improvements.

Acknowledgments

This work was made in the framework of the ANR funded project ANR-20-CE29-0022, SQLX "Spectroscopy and quantification of lithium by x-ray microanalysis", https://anr.fr/Projet-ANR-20-CE29-0022.

Nicolas Brodusch from McGill University in Montréal, Canada, is thanked for sharing his knowledge and technique to etch quasi-crystals. Rabah Benbalagh from LCPMR is thanked for performing the etching of the sample. Vincent Fournée, from Institut Jean Lamour in Nancy, France, is thanked for giving the experimental conditions used in Ref. [26]. We also extend our gratitude to Aurélien Moy from the University of Wisconsin-Madison for his invaluable assistance and help with the quantification code.

Licence

Bibliography

[1] M. Terauchi, M. Kawana, Soft-X-ray emission spectroscopy based on TEM—Toward a total electronic structure analysis, Ultramicroscopy 106 (2006) 1069–1075. https://doi.org/10.1016/j.ultramic.2006.04.021.

[2] A. Erko, A. Firsov, R. Gubzhokov, A. Bjeoumikhov, A. Günther, N. Langhoff, M. Bretschneider, Y. Höhn, R. Wedell, New parallel wavelength-dispersive spectrometer based on scanning electron microscope, Opt. Express 22 (2014) 16897. https://doi.org/10.1364/OE.22.016897.
[3] M. Terauchi, H. Takahashi, N. Handa, T. Murano, M. Koike, T. Kawachi, T. Imazono, M. Koeda, T. Nagano, H. Sasai, Y. Oue, Z. Yonezawa, S. Kuramoto, Ultrasoft-X-ray emission spectroscopy using a newly designed wavelength-dispersive spectrometer attached to a transmission electron microscope, J. Electron Microsc. (Tokyo) 61 (2012) 1. https://doi.org/10.1093/jmicro/dfr076.
[4] C.M. MacRae, A.E. Hughes, J.S. Laird, A.M. Glenn, N.C. Wilson, A. Torpy, M.A. Gibson, X. Zhou, N. Birbilis, G.E. Thompson, An Examination of the Composition and Microstructure of Coarse Intermetallic Particles in AA2099-T8, Including Li Detection, Microsc. Microanal. 24 (2018) 325–341. https://doi.org/10.1017/S1431927618000454.
[5] K. Hassebi, N. Rividi, M. Fialin, A. Verlaguet, G. Godard, J. Probst, H. Löchel, T. Krist, C. Braig, C. Seifert, R. Benbalagh, R. Vacheresse, V. Ilakovac, K.L. Guen, P. Jonnard, High-resolution x-ray emission spectrometry in the lithium K range with a reflection zone plate spectrometer, X-Ray Spectrom. n/a (2024). https://doi.org/10.1002/xrs.3427.
[6] J.-L. Pouchou, Les méthodes de quantification en microanalyse X, in: Microsc. Électronique À Balayage Microanal., EDP Sciences, F. Brisset, Paris, 2008. http://www.edition-sciences.com/microscopie-electronique-a-balayage-et-microanalyses.htm (accessed December 4, 2013).
[7] X. Llovet, P. Pöml, A. Moy, J.H. Fournelle, Assessing the accuracy of mass attenuation coefficients for soft X-ray EPMA, Microsc. Microanal. 29 (2023) 540–551. https://doi.org/10.1093/micmic/ozac045.
[8] P. Schweizer, Y. Ménesguen, M.-C. Lépy, E. Brackx, M. Duchateau, P. Jonnard, High-accuracy experimental determination of photon mass attenuation coefficients of transition metals and lithium fluoride in the ultra-soft energy range, Phys. Chem. Chem. Phys. (2024). https://doi.org/10.1039/D4CP00500G.
[9] H.H. Johann, Die Erzeugung lichtstarker Röntgenspektren mit Hilfe von Konkavkristallen, Z. Für Phys. 69 (1931) 185–206. https://doi.org/10.1007/BF01798121.
[10] L.V. Azaroff, X-ray Spectroscopy, McGraw-Hill Inc., New York, 1974.
[11] Reflection zone plates, Nanooptics-Berl. (n.d.). https://www.nanooptics-berlin.com/reflection-zone-plates (accessed May 6, 2024).
[12] D. Shechtman, I. Blech, D. Gratias, J.W. Cahn, Metallic phase with long-range orientational order and no translational symmetry, Phys. Rev. Lett. 53 (1984) 1951–1953. https://doi.org/10.1103/PhysRevLett.53.1951.
[13] S.J. Poon, Electronic properties of quasicrystals an experimental review, Adv. Phys. 41 (1992) 303–363. https://doi.org/10.1080/00018739200101513.
[14] E. Belin-Ferré, Z. Dankhazi, M.F. Fontaine, M.C. de Weerd, J.M. Dubois, Electronic densities of states and pseudo-gaps in Al-based complex intermetallics, Croat. Chem. Acta 83 (2010) 55–58.
[15] A. Janner, Crystallography of Quasicrystals, in: A. Amann, L.S. Cederbaum, W. Gans (Eds.), Fractals Quasicrystals Chaos Knots Algebr. Quantum Mech., Springer Netherlands, Dordrecht, 1988: pp. 93–109. https://doi.org/10.1007/978-94-009-3005-6_6.
[16] R. Gauvin, P. Michaud, MC X-Ray, a new Monte Carlo program for quantitative X-Ray microanalysis of real materials, Microsc. Microanal. 15 (2009) 488–489. https://doi.org/10.1017/S1431927609092423.
[17] CXRO X-Ray Interactions With Matter, X-Ray Interact. Matter (n.d.). http://henke.lbl.gov/optical_constants/ (accessed January 30, 2014).
[18] J.-L. Pouchou, F. Pichoir, Quantitative Analysis of Homogeneous or Stratified Microvolumes Applying the Model “PAP,” in: K.F.J. Heinrich, D.E. Newbury (Eds.), Electron Probe Quant., Springer US, Boston, MA, 1991: pp. 31–75. https://doi.org/10.1007/978-1-4899-2617-3_4.
[19] A. Moy, J. Fournelle, φ(ρz) distributions in bulk and thin film samples for EPMA. Part 1: A modified φ(ρz) distribution for bulk materials, including characteristic and Bremsstrahlung

fluorescence, Microsc. Microanal. 27 (2021) 266–283. https://doi.org/10.1017/S1431927620024915.
[20] K.F.J. Heinrich, Mass absorption coefficients for electron probe microanalysis, in: J.D. Brown, R.H. Packwood (Eds.), Proc. 11th Int. Conf. X-Ray Opt. Microanal., University of Western Ontario Press, London, Ontario, 1987: pp. 67–119.
[21] C.T. Chantler, Detailed tabulation of atomic form Factors, photoelectric absorption and scattering cross section, and mass attenuation coefficients in the vicinity of absorption edges in the soft X-Ray (Z=30–36, Z=60–89, E=0.1 keV–10 keV), addressing convergence issues of earlier work, J. Phys. Chem. Ref. Data 29 (2000) 597–1056. https://doi.org/10.1063/1.1321055.
[22] D.E. Cullen, J.H. Hubbell, L. Kissel, EPDL97: the Evaluated Photon Data Library, 1997.
[23] L. Sabbatucci, F. Salvat, Theory and calculation of the atomic photoeffect, Radiat. Phys. Chem. 121 (2016) 122–140. https://doi.org/10.1016/j.radphyschem.2015.10.021.
[24] D.E. Cullen, EPICS2023: Electron Photon Interaction Cross Sections (2023), (n.d.). https://www-nds.iaea.org/epics/ (accessed May 13, 2024).
[25] P.A. Bruhwiler, J.L. Wagner, B.D. Biggs, Y. Shen, K.M. Wong, S.E. Schnatterly, S.J. Poon, Soft-x-ray, heat-capacity, and transport measurements on icosahedral and crystalline alloys, Phys. Rev. B 37 (1988) 6529–6532. https://doi.org/10.1103/PhysRevB.37.6529.
[26] E. Belin, Z. Danhkázi, Valence band electronic distributions in quasicrystals, J. Non-Cryst. Solids 153–154 (1993) 298–302. https://doi.org/10.1016/0022-3093(93)90361-Z.
[27] T. Fujiwara, T. Yokokawa, Universal pseudogap at the Fermi energy in quasicrystals, Phys. Rev. Lett. 66 (1991).
[28] T. Fujiwara, G. Trambly de Laissardière, S. Yamamoto, Electronic structure and transport properties in quasi-crystals, Mater. Sci. Eng. A 179–180 (1994) 118–121. https://doi.org/10.1016/0921-5093(94)90176-7.
[29] P. Jonnard, C. Bonnelle, Cauchois and Sénémaud Tables of wavelengths of X-ray emission lines and absorption edges, X-Ray Spectrom. 40 (2011) 12–16. https://doi.org/10.1002/xrs.1293.
[30] R. v. Baltz, Plasmons and Surface Plasmons in Bulk Metals, Metallic Clusters, and Metallic Heterostructures, in: B. Di Bartolo, S. Kyrkos (Eds.), Spectrosc. Dyn. Collect. Excit. Solids, Springer US, Boston, MA, 1997: pp. 303–338. https://doi.org/10.1007/978-1-4615-5835-4_11.
[31] K. Mukai, R. Kasada, K. Sasaki, S. Konishi, Occupied Electronic States of Li in Li, Li2O2, and Li2O Analyzed by Soft X-ray Emission Spectroscopy, J. Phys. Chem. C 124 (2020) 9256–9260. https://doi.org/10.1021/acs.jpcc.0c02885.
[32] K. Hassebi, K. Le Guen, N. Rividi, A. Verlaguet, P. Jonnard, Calculation of emission spectra of lithium compounds, X-Ray Spectrom. 52 (2023) 330–335. https://doi.org/10.1002/xrs.3329.
[33] M.A. Markus, W. Elser, T2-AlLiCu: A stable icosahedral phase?, Phil. Mag. B 54 (1986) L101-L104. https://doi.org/10.1080/13642818608239018.
[34] M. de Boissieu, C. Janot, J.-M. Dubois, M. Audier, B. Dubost, Atomic structure of the icosahedral Al-Li-Cu quasicrystal, J. Phys. Cond. Matter 3, (1991) 1. https://doi.org/ 10.1088/0953-8984/3/1/001
[35] P. Donnadieu, K. Wang, C. Degand, P. Garoche, Improving the Al6Li3Cu quasicrystals by annealing treatments, J. Non-crystalline solids 183, (1995): 100-108. https://doi.org/10.1016/0022-3093(94)00559-1.

MAC database	*Ultra-soft x-ray range*		
	Al (wt%) / (at%)	*Li (wt%)/ (at%)*	*Cu (wt%)/ (at%)*
MAC30	74.2 / 52.7	16.2 / 44.5	9.4 / 2.8
Chantler	49.6 / 35.6	19.8 / 55.1	30.5 / 9.3
EPDL97	51.2 / 37.2	19.1 / 53.7	29.6 / 9.1
PENELOPE 2018	57.3 / 39.1	20.7 / 54.6	21.9 / 6.3
EPDL 2023	63.8 / 51.6	12.9 / 40.4	23.2 / 8.0
	Soft x-ray range		
MAC30	59.6 / 44.1	16.9 / 48.3	23.5 / 7.5

Table 1: Weight fractions for the AlCuLi quasi-crystal calculated from the Li Kα and Al $L_{2,3}$ intensities and with MAC from different databases. The Cu weight fraction is determined by difference. The last line gives the weight fractions determined from the Al Kα and Cu Lα intensities in the soft x-ray range. In this case, the Li weight fraction is calculated by difference.